

## Image-guided $^{31}\text{P}$ magnetic resonance spectroscopy of normal and transplanted human kidneys

MICHAEL D. BOSKA, DIETER J. MEYERHOFF, DONALD B. TWIEG, GREGORY S. KARZMAR, GERALD B. MATSON, and MICHAEL W. WEINER

Magnetic Resonance Unit, Veterans Administration Medical Center; Philips Medical Systems; the Departments of Medicine, Radiology, and Pharmaceutical Chemistry, University of California, San Francisco, San Francisco, California, USA

**Image-guided  $^{31}\text{P}$  magnetic resonance spectroscopy of normal and transplanted human kidneys.** Image-guided  $^{31}\text{P}$ -phosphorus magnetic resonance spectroscopy (MRS) was used to obtain spatially localized  $^{31}\text{P}$  spectra of good quality from healthy normal human kidneys and from well-functioning renal allografts. A surface coil of 14 cm diameter was used for acquiring phosphorus signals solely from a volume-of-interest located within the kidney. To determine the effects of kidney transplantation on renal metabolism, patients with well functioning allografts were studied. Little or no phosphocreatine in all spectra verifies the absence of muscle contamination, and is consistent with proper volume localization. The intensity ratio of phosphomonoesters (PME) to adenosine triphosphate (ATP) resonances in transplanted kidneys (PME/ATP =  $1.1 \pm 0.4$ ) was slightly elevated ( $P = 0.2$ ) compared to that of healthy normal kidneys (PME/ATP =  $0.8 \pm 0.3$ ). The inorganic phosphate (Pi) to ATP ratio was similar in the two groups (Pi/ATP =  $1.1 \pm 0.1$  in transplanted kidneys vs.  $1.2 \pm 0.6$  in normal kidneys). Acid/base status, as evidenced from the chemical shift of Pi, was the same in both normal controls and transplanted kidneys. Despite the practical problems produced by organ depth, respiratory movement, and tissue heterogeneity, these results demonstrate that image-guided  $^{31}\text{P}$  MR spectra can reliably be obtained from human kidneys.

A high rate of oxidative phosphorylation in the kidney is needed to maintain a stable concentration of adenosine triphosphate (ATP), which is used in part to provide the energy for the solute reabsorption taking place in the renal tubules. Thus, pathophysiological conditions which suppress oxidative phosphorylation, such as renal ischemia, may be associated with a diminished concentration of ATP [1] and tissue acidosis [2]. The method of  $^{31}\text{P}$  magnetic resonance spectroscopy ( $^{31}\text{P}$  MRS) enables non-invasive measurement of phosphorus metabolites including ATP, inorganic phosphate (Pi), phosphodiester (PDE) including glycerophosphorylcholine and glycerophosphorylethanolamine, and phosphomonoesters (PME) including phosphorylcholine and phosphorylethanolamine. Several reviews concerning MRS studies of kidney metabolism in animals have been recently published [3-6].

The use of  $^{31}\text{P}$  MRS to study renal metabolism was initiated by Sehr et al [7], who obtained phosphorus signals from isolated

kidneys in vitro. Subsequently, Ackerman et al [8] investigated the effects of acute acidosis using the isolated, perfused kidney. Weiner and colleagues [9 and literature cited therein] studied high-energy phosphate metabolism of the intact kidney in situ using implanted radio frequency coils, and found that acute ischemia caused rapid disappearance of ATP [10] accompanied by a rise of Pi. Siegel and coworkers [11] have studied the effects of renal ischemia in situ using acutely implanted radio frequency coils, and found that alterations of high-energy phosphates correlated closely with recovery of renal function. Balaban, Gadian and Radda [12] first measured renal  $^{31}\text{P}$  MRS signals from an intact animal without implanted coils, using topical magnetic resonance.

The availability of whole-body, high field magnets for magnetic resonance imaging (MRI), along with the recent development of improved localization techniques [13-18] have permitted MRS investigations of human brain, liver and heart [reviewed in 19, 20]. However, the normal kidney has been a particularly difficult organ for MRS studies for several reasons: First, the kidney is at a greater distance from the surface of the body than the previously studied organs, and a thick layer of muscle lies between the body surface and the kidney. Second, the kidney may move with respiration, making it difficult to obtain MR spectra localized solely in the kidney during the long spectral acquisition time. Finally, the presence of different internal structures within the kidney (cortex, medulla, hilum) complicates interpretation of spectra obtained from the entire organ. Despite these problems, MRS studies of the human kidney in situ are of potential importance because they are expected to provide insight into the metabolic disturbances associated with alterations of normal physiology, kidney disease, and renal transplantation.

The goal of the present experiments was to implement a spatially localized technique so that  $^{31}\text{P}$  MR kidney spectra could be routinely obtained without significant contamination from surrounding tissues. Recent computer simulation studies have indicated the ability of the ISIS localization method to achieve satisfactory localization with surface coils [21]. In addition, in preliminary MRS localization experiments we have demonstrated our ability to obtain  $^{31}\text{P}$  spectra from normal human kidney using ISIS [22]. Thus, the present studies were initiated with a series of  $^{31}\text{P}$  MRS measurements on normal human subjects. In order to determine the effects of kidney

transplantation on renal metabolism, several patients with well-functioning allografts were also studied.

## Methods

### *Volunteers and patients*

A total of 14 healthy volunteers (9 male, 5 female), 21 to 59 years of age, and 6 male patients, 24 to 67 years of age, participated in the study. Only volunteers with no known history of kidney disease, and whose scout MR images showed no evidence of renal abnormalities, were selected. All patients selected had kidney transplants functioning well for more than one year as indicated by standard laboratory tests, and patients showed no clinical evidence of urinary obstruction. In addition, scout MR images obtained at the time of the MRS examination showed no renal abnormalities. Spectra with a sufficient signal-to-noise ratio (S/N) to reliably determine peak integrals were obtained from seven volunteers and five transplant patients. Kidney spectra from 10 volunteers and 6 transplant patients were used to determine average chemical shifts of  $^{31}\text{P}$  metabolites. The success rate with which spectra from normal kidneys were obtained increased significantly with the introduction of shim routines that allowed shimming localized solely on kidney tissue. The study had prior approval from the UCSF Committee of Human Research and informed consent was obtained from every subject before examination.

### *Magnetic resonance instrumentation and measurements*

$^{31}\text{P}$  MR spectra were obtained with a Philips Gyroscan system operating at 2.0 Tesla (34.78 MHz for  $^{31}\text{P}$ ) and equipped with a spectroscopy package (Philips Medical Systems, The Netherlands). Subjects were studied with the surface coil placed underneath the kidney. In this position the surface coil was orthogonal to the  $B_1$  field of the imaging body coil, which minimized RF interactions. A balanced matched [23], single-turn surface coil of 14 cm diameter was used for transmitting and receiving. A small glass vial containing 3 ml of hexamethylphosphorotriamide (HMPT,  $\text{P}[\text{N}(\text{CH}_3)_2]_3$ ), placed at the center of the surface coil, served to identify coil position on the locator MR image, and to calibrate the  $^{31}\text{P}$  RF field strength at the center of the coil (so that the  $90^\circ$  pulse length at the center of the VOI could be determined with computer-generated  $B_1$  field plots [21]). A similar glass vial containing tributylphosphine [TBP,  $\text{P}(\text{OC}_4\text{H}_9)_3$ ], which resonates 16 ppm downfield from HMPT, was placed next to the HMPT vial to aid in the determination of phasing parameters for  $^{31}\text{P}$  spectra.

*Examination procedure.* Normal subjects were positioned supine, and transplant patients positioned prone, with the kidney centered over the surface coil. A gap of about 1 cm was maintained between the surface coil and the subject's skin. Proton MR images were obtained using a Philips body coil. Standard spin echo imaging techniques were employed without respiratory gating to obtain scout (locator) images. A Gordon-Timms arrangement [24] for double tuning the surface coil to the proton frequency was used for shimming the magnet on the  $^1\text{H}$  signal of the tissue water. With a DEPTH-pulse shim sequence [25], optimized to suppress muscle and fat signal from tissue close to the coil, water linewidths of 20 to 35 Hz were achieved routinely in 5 to 15 minutes. For some studies a stimulated echo technique (STEVE) [26] was used to shim on

the VOI used for the  $^{31}\text{P}$  ISIS acquisition. This technique yielded typical linewidths of 10 Hz. The frequency was then switched to 34.78 MHz for  $^{31}\text{P}$  (with the carrier placed between the HMPT and TBP resonances at ca. 137 ppm downfield from  $\gamma\text{-ATP}$ ) and the  $180^\circ$  pulse length of the HMPT phantom was determined (between 100 and 180  $\mu\text{s}$ ). From this calibration the  $90^\circ$  plus length at the center of the VOI was calculated (between 140 and 200  $\mu\text{s}$ ) using computer simulated  $B_1$  isocontours of the surface coil [21]. A one-pulse, fully relaxed spectrum of the HMPT and TBP samples was stored for determination of zero and first order phasing parameters. The proton images were used to determine: 1) the coordinates of the VOI with respect to the isocenter of the magnet; 2) the position of the VOI with respect to the surface coil, usually centered about 50 mm from the surface coil for transplanted kidney and 70 mm for normal kidney studies; and 3) the volume of the VOI, usually between 30 and 60 ml.  $^{31}\text{P}$  spectra were then acquired with the carrier placed between the  $\gamma\text{-ATP}$  and PDE resonances. A modified ISIS localization technique was used to reduce acquisition of signal from outside the VOI produced by rapid signal averaging [21, 22]. The following acquisition parameters were used: pulse repetition time (TR) = 2 s, data size = 512 points, spectral width = 3000 Hz, number of signal averages = 600 to 2700.

### *Data analysis*

Spectral data were processed using the NMR1 software package (New Methods Research, Inc., New York, USA) on a VAX 11/730 and SUN 3/110. To obtain reliable integration of the peak areas, the broad spectral component that underlies narrower metabolite peaks was removed by convolution difference. (The broad spectral component is due to less mobile phospholipids, bound phosphorus compounds and, possibly, paramagnetically broadened components.) The raw FID was multiplied with an exponential line-broadening factor of 300 Hz which corresponded roughly to the linewidth-at-half-height of the broad component in our experiments. Eighty percent of this spectral component was then subtracted from the raw FID to give  $\text{FID}^{\text{cd}} = \text{FID}^{\text{raw}} \times (1 - 0.8 \exp(-300 \pi t))$ .  $\text{FID}^{\text{cd}}$  was then multiplied with an exponential line-broadening factor of 20 Hz, zero-filled to 1K data size and Fourier transformed.

*Phasing.* Correct phasing of low S/N spectra is critical for peak integration, but is operator dependent. Therefore, in the present experiments a one-pulse spectrum obtained from the HMPT and TBP standards was not only used to calibrate pulse power, but also to determine phase parameters for spectra obtained from human kidneys. The high S/N of such a one-pulse spectrum (typically around 50) allowed precise determination of phasing parameters. Employment of these phasing standards made phasing reproducible and independent of operator bias. In vivo spectra obtained this way usually showed a flat baseline after application of the convolution difference and were taken as input for the curve fit routine which provided automatic signal integration.

*Signal integration.* Figure 1 demonstrates the iterative curve fitting routine of NMR1 used to integrate the six major metabolite peaks in a typical kidney transplant spectrum. Figure 1A shows the difference between the experimental and computer generated spectra. Figure 1B displays the original baseline flattened spectrum. Figure 1C is a computer generated spectrum; it is displayed deconvoluted into its individual Gaussian

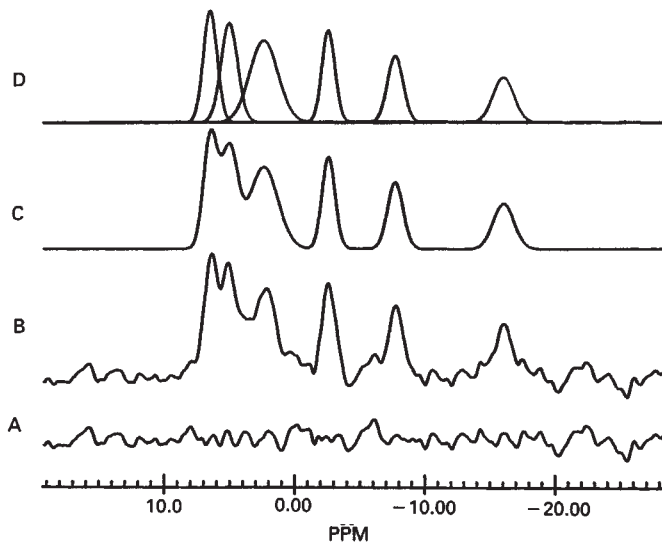


**Fig. 1.** Result of spectral curve fitting and integration. A. Difference between the actual data and the calculated fit; B. spectrum obtained from a transplanted human kidney; C. NMR1 fit to the entire spectrum; D. deconvolution of the individual peaks in the spectrum which was used for integration of the individual spectral components.

signal components in Figure 1D. These components were integrated individually  $\pm 5$  linewidths around their resonance frequency. The difference spectrum in Figure 1A demonstrates the good spectral fit. The  $\gamma$ -ATP peak area was used for deriving metabolite ratios containing ATP with the premise that ADP in kidney is undetectable by MRS [27]. The  $\alpha$ -ATP peak area contains contributions from nicotinamide adenine dinucleotides (such as, NAD, NADH and their phosphates). The  $\beta$ -ATP peak intensity was not used to derive ratios as it was decreased significantly in these surface coil ISIS experiments due to the "chemical shift offset effect" [for a discussion of this effect see ref. 21 and 28].

**Chemical shift.** Chemical shifts are reported relative to  $\alpha$ -ATP at  $-7.66$  ppm. Reported values in ppm are derived from curve-fitted spectra.

#### Statistical analysis

Statistical significance of the results was determined by use of the unpaired *t*-test. A *P*-value of less than 0.05 was considered significant. Values are expressed as mean  $\pm$  SD.

#### Results

##### $^1\text{H}$ MRI of normal and transplanted human kidneys

Figure 2 shows spin echo MR images obtained without respiratory gating from 10 mm thick slices with the whole body MRI coil. These scout images were used to locate the kidneys and define the coordinates for the VOI from which  $^{31}\text{P}$  spectra were acquired. The overall image quality, particularly the sharp outline, indicates relatively little respiratory motion of the kidneys. Nevertheless, cortico-medullary differentiation [29] is poor. Figure 2A shows the two normal kidneys of a 59-year-old male volunteer. Figure 2B shows a MR image of a 52-year-old male with a renal transplant (subject #2) whose laboratory tests indicated a well functioning allograft. On both Figures 2A and

2B the rectangular boxes indicate the anatomical region from which the  $^{31}\text{P}$  MR spectra were obtained (ISIS VOI). While each MR image depicts a single 10 mm thick slice through the center of the ISIS VOI, the total VOI extends typically over 35 to 50 mm. The boxes indicate a nominal VOI; the acquired  $^{31}\text{P}$  signals actually originate from a slightly larger volume than indicated by the nominal ISIS box [21].

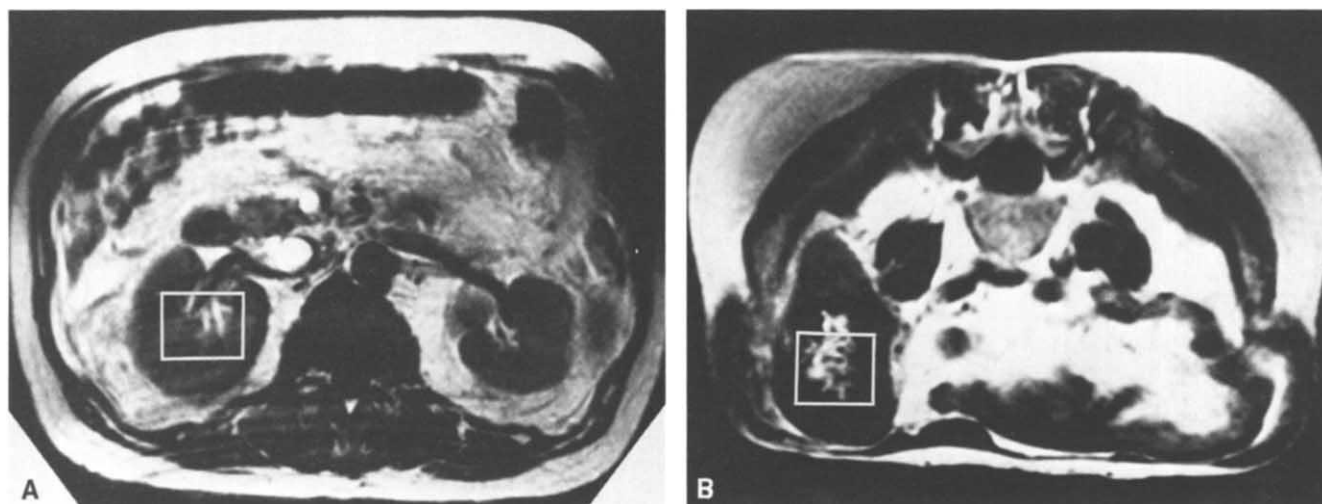
##### $^{31}\text{P}$ MRS of normal and transplanted human kidneys

Figure 3A shows a typical  $^{31}\text{P}$  MRS spectrum of a normal kidney obtained with the ISIS localization technique with a one hour acquisition time. Six major peaks were detected including phosphomonoesters (PME), inorganic phosphate (Pi), phosphodiester (PDE), and the  $\gamma$ -,  $\alpha$ -, and  $\beta$ -resonances of adenosine triphosphate. The peak labelled PDE may also contain some signal contribution from phosphate in urine [30]. However, in contrast to animal kidneys [30], none of the kidney spectra showed a discernable narrow peak in the PDE region typical for urinary Pi. Only a very small peak for phosphocreatine (PCr) can be seen, indicating lack of significant contamination of signal from surrounding skeletal or smooth muscle. The  $\beta$ -ATP resonance is significantly smaller than the  $\gamma$  ATP resonance; this is due to the "chemical shift offset effect" in which the VOI for the  $\beta$ -ATP is shifted slightly further from the coil than the other resonances [21, 28]. The S/N ratio measured on Pi is 7.5, while S/N in the analyzed normal kidney spectra varied between 4.5 and 9 (mean 6.5,  $N = 7$ ).

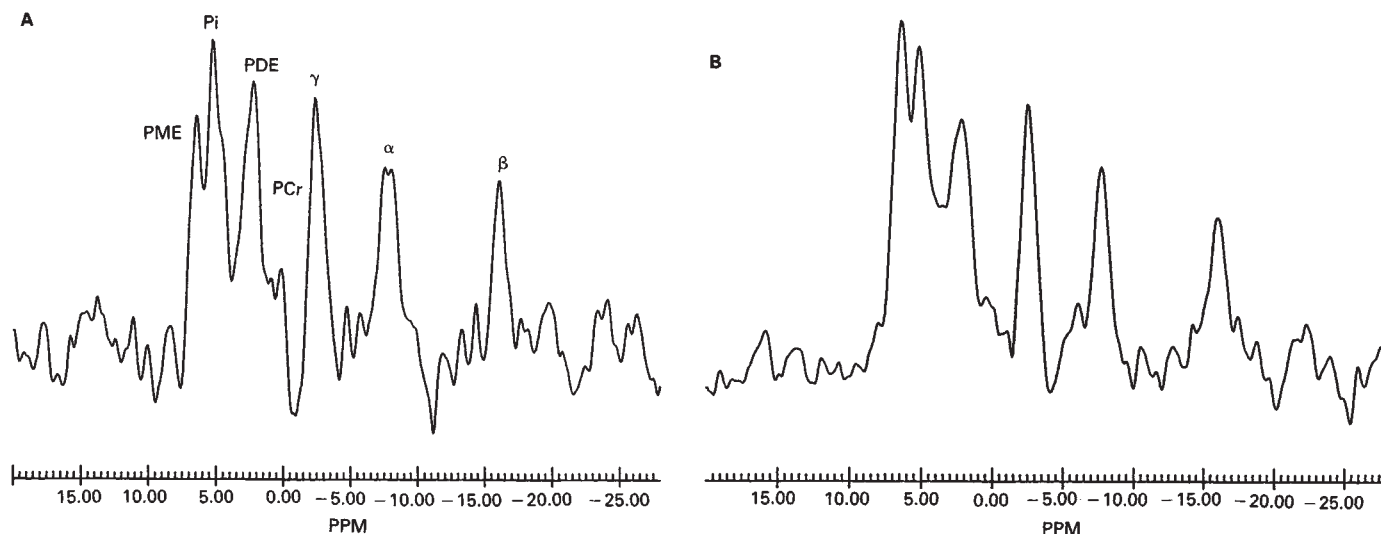
Figure 3B shows the  $^{31}\text{P}$  ISIS spectrum obtained in a one hour acquisition time from the renal allograft depicted in Figure 2B. Peaks for the same six resonances seen in the normal kidney are visible. Almost no PCr is detected. The height of the PME peak is greater than that seen in the normal kidney. Similar to the normal kidney, the  $\beta$ -ATP peak is smaller than the  $\alpha$ - or  $\gamma$ -ATP peaks, due to the "chemical shift offset effect". The S/N measured on Pi is 9.1, while S/N in the analyzed kidney transplant spectra varied between 4.6 and 10.5 (mean 6.5,  $N = 5$ ).

Table 1 shows the clinical and MRS data from each of the kidney transplant patients studied. The PME/ATP and Pi/ATP ratios are shown for each patient. There was no correlation between these MRS data and blood urea nitrogen (BUN), creatinine, blood pressure, or medication. The average PME/ATP ratio of the normal kidneys was  $0.8 \pm 0.3$ . The PME/ATP ratio of the transplanted kidneys ( $1.1 \pm 0.4$ ) was slightly increased compared to normal kidneys, though the increase was not statistically significant ( $P = 0.244$ ). The Pi/ATP ratio of the normal kidneys was  $1.2 \pm 0.6$ , compared to  $1.1 \pm 0.1$  in the transplanted kidneys. The PME/Pi and PDE/ATP ratios were not significantly different between the two groups.

Chemical shifts in ppm for the major metabolites in 10 normal kidneys measured relative to  $\alpha$ -ATP at  $-7.66$  ppm were: PME  $6.69 \pm 0.15$ , Pi  $5.25 \pm 0.26$ , PDE (including any possible urinary Pi)  $2.80 \pm 0.45$ ,  $\gamma$ -ATP  $-2.39 \pm 0.18$ ,  $\beta$ -ATP  $-16.00 \pm 0.14$  (mean  $\pm$  SD). These values were not significantly different from values obtained from the six kidney transplants. Pi chemical shift in transplants was also  $5.25 \pm 0.14$  ppm. Absolute renal pH was not calculated from the Pi chemical shift due to the lack of a suitable chemical shift reference or titration curve. The water resonance in renal tissue was not used as internal chemical shift



**Fig. 2.** A. Locator MR scout image of healthy normal human kidneys. Acquisition parameters: TR = 450 ms, TE = 30 ms, FOV = 400 mm, slice thickness = 10 mm, 1 measurement. The outlined box indicates the region of interest selected for spectral acquisition. B. Locator MR scout image of a renal transplant with the outlined box indicating the region of interest selected for spectral acquisition. Acquisition parameters as in A.



**Fig. 3.**  $^{31}\text{P}$  ISIS spectra of the healthy normal kidney (A) seen in Figure 2A, and of the well functioning kidney transplant (B) shown in Figure 2B. Acquisition parameters: TR = 2.0 s, acquisition time = 1 hr, 90 degree pulse set for the region of interest, distance of the center of VOI from 14 cm surface coil = 70 mm for normal kidney and 42 mm for transplanted kidney, size of the VOI  $25 \times 45 \times 55$  mm = 62 ml for normal kidney and  $25 \times 50 \times 54$  mm = 68 ml for transplanted kidney.

reference [31] because of the presence of residual eddy currents in the ISIS experiment which could lead to frequency shifts.

### Discussion

Researchers in several laboratories have been performing image-guided  $^{31}\text{P}$  MRS studies of human organs over the past several years [28, 32–38]. In this laboratory we have been using MR localization techniques routinely to obtain  $^{31}\text{P}$  MR spectra from human muscle [35], brain [35, 36], liver [22, 28, 37], and heart [22, 38]. However, the only  $^{31}\text{P}$  spectra of normal human kidneys reported thus far are a single spectrum by Jue et al [39] and an ISIS spectrum obtained previously in this laboratory [22].  $^{31}\text{P}$  spectra from well functioning renal allografts were previously reported in an abstract [40] using  $^{31}\text{P}$  DRESS local-

ization techniques. The depth of the normal kidney and respiratory movement have greatly hampered acquisition of spectra from normal kidneys without substantial contamination of signal from surrounding muscle. Initial studies of normal kidneys in this laboratory were not very successful because of these problems and because of difficulties shimming over the kidney volume. Recently, our ability to obtain kidney spectra improved, largely because of two reasons: First, minimization of kidney respiratory movement by supine positioning of normal controls; second, the ability to perform shimming localized with stimulated echo techniques [26].

This report describes the first  $^{31}\text{P}$  MRS study of the metabolic characteristics of healthy normal and transplanted kidneys in human subjects. The present results demonstrate that  $^{31}\text{P}$  MR

**Table 1.** Clinical and MRS data of kidney transplant patients

Patient no.	BUN <sup>a</sup>	Creatinine <sup>b</sup>	Blood pressure	CSA <sup>c</sup> μg/liter	Prednisone	Azathioprine	PME/ATP	Pi/ATP
	mg/dl	mg/dl			mg/day	mg/day		
1	21	1.3	132/90	350	10	—	1.7	1.2
2	40	2.0	150/90	80	10	75	0.8	1.0
3	14	1.3	125/80	275	10	—	1.5	1.0
4	21	1.9	167/70	100	7.5	50	0.7	1.2
5	21	2.3	130/80	325	10	75	0.7	0.9

<sup>a</sup> normal range: 10 to 24<sup>b</sup> normal range: 0.6 to 1.4<sup>c</sup> whole blood HPLC method**Table 2.** Metabolite ratios and Pi chemical shift ( $\delta$ ) in normal and transplanted human kidneys (mean  $\pm$  SD)

Ratios	Normal <i>N</i> = 7	Transplanted <i>N</i> = 5
PME/ATP	0.8 $\pm$ 0.3	1.1 $\pm$ 0.4
Pi/ATP	1.2 $\pm$ 0.6	1.1 $\pm$ 0.1
PME/Pi	0.9 $\pm$ 0.6	1.0 $\pm$ 0.3
PDE/ATP	2.6 $\pm$ 1.2	1.8 $\pm$ 0.7
$\delta_{\text{Pi}}$ [ppm]	5.25 $\pm$ 0.26 <sup>a</sup>	5.25 $\pm$ 0.14 <sup>b</sup>

<sup>a</sup> *N* = 10<sup>b</sup> *N* = 6

spectra with adequate S/N and resolution can be regularly obtained from normal human kidneys. Signal-to-noise per unit time, however, is reduced compared to that of kidney transplant spectra, because normal kidneys are usually located deeper inside the body than allografts, and thus further away from the receiver surface coil. However, spectra obtained in this study from normal kidneys show little or no signal from phosphocreatine, demonstrating that the spectra are not significantly contaminated by signal from surrounding skeletal muscle or smooth muscle of the intestines, and indicating that the spectra represent renal tissue.

The spectra obtained from normal human subjects and transplant recipients are very similar to those previously reported from animal kidneys using a variety of techniques [41, 42]. In comparison to other normal tissues, except for brain [36], normal kidneys showed relatively large peaks for PME. The PME/ATP ratio for normal kidney was 0.8, while PME/ATP was 0.3 in liver [37] and <0.1 in muscle [35]. Based on  $^{31}\text{P}$  chemical shift (6.69  $\pm$  0.15 ppm) this high PME peak probably represents phosphorylethanolamine [3], which is the major component of the PME peak in other tissues [36, 37, 43]. It was previously demonstrated that the relatively narrow resonance signal from phosphate in tubular fluid in the renal pelvis overlaps with the PDE peak [30, 44–46]. A significant contribution of urinary Pi to the PDE resonance is expected with any degree of urinary obstruction, causing dilatation of the calyces with a concomitant increase in amount of urine within the measured volume. However, in this study there was no clinical or MRI evidence of obstruction in any of the studied subjects, and no discernable narrow peak in the PDE region, characteristic for urinary Pi, was observed. Therefore, the broad PDE peak is most likely composed of glycerophosphorylcholine and glycerophosphorylethanolamine.

The PME/ATP ratio in renal transplants was slightly higher

than in healthy normal kidneys, although this difference was not statistically significant. However, we note that previous studies of transplanted kidneys in rats have shown elevated PME/ATP ratios in rejecting kidneys [41].

The Pi/ATP in the well-functioning renal transplants studied was comparable to that in normal kidneys, and similar to that found in well-functioning rat kidney allografts [41]. However, in the rat, rejection was associated with an increased Pi/ATP ratio, possibly due to ischemia [41]. An increased Pi/ATP ratio in human transplants might also suggest renal ischemia due to rejection or effects of cyclosporin A [41, 42].

There are a number of problems associated with  $^{31}\text{P}$  MRS of the normal and transplanted human kidney. Most of these problems relate to the low sensitivity of the experiment in part due to the relatively small renal tissue volume and the depth of the kidney from the surface. It is for these reasons that spectra from renal transplants can be obtained with higher S/N than spectra from normal kidneys. This low sensitivity of the experiment limited the number of successful studies to only 7 out of 14 normal subjects, and it necessitated a minimum acquisition time of 30 minutes for normal kidneys. Low S/N also prevented acquisition of spectra from specific zones of the kidney, such as renal cortex and medulla. The localized  $^{31}\text{P}$  spectra obtained in this study consist of signals from primarily medulla and cortex, even though the nominal ISIS volume depicted in Figure 2 is centered over the renal pelvis. Blood and urine occupy a small percentage of the true ISIS volume and contain low concentrations of phosphorylated metabolites; therefore it is probable that they did not contribute significantly to  $^{31}\text{P}$  spectra. Despite the fact that spectra were obtained from heterogeneous tissue, we think that spectra obtained from normal and transplanted kidneys can be compared because all ISIS VOI's are similarly composed of the three renal structures. Because of the probability that the Pi peak originates from inorganic phosphate in different compartments [3] we do not calculate intrarenal pH. However, it is noteworthy that the mean Pi chemical shift is the same in both normal and transplanted kidney (5.25 ppm), while the relatively large standard deviation ( $\pm$  0.14 and  $\pm$  0.26 ppm) may indicate signal heterogeneity. As more sensitive techniques are developed, and higher-field magnets come into use,  $^{31}\text{P}$  MRS may ultimately detect localized signals from specific zones of the kidney.

These findings demonstrate the feasibility of performing localized magnetic resonance spectroscopy of the human kidney, and suggest that there are no significant differences between metabolite ratios of normal kidneys and well-functioning kidney transplants, if spectra are obtained from the whole

kidney. Furthermore, these findings suggest that the non-invasive MRS technique may be used to assess alterations of overall renal pH in various acid-base disturbances [46, 47] and changes in renal ATP associated with ischemic renal failure as observed in previous animal studies [9, 11, 12]. The present finding that renal transplants may have slightly increased PME raises the possibility that  $^{31}\text{P}$  MRS may be useful to assess changes in renal metabolism associated with transplantation. Future studies will be aimed at improving spatial resolution to obtain spectra from different regions of the kidney and at determining the effects of rejection and cyclosporine nephrotoxicity on renal metabolism. In addition to  $^{31}\text{P}$  MR spectra, investigators have obtained  $^1\text{H}$  metabolite spectra of other human organs using water suppression techniques [for example, 48–50] and also natural abundance  $^{13}\text{C}$  spectra [such as, 51]; in principle these methods could also be applied to kidney. Ultimately, the information obtained from localized MRS studies of the human kidney may provide additional insights into alterations of renal metabolism associated with physiological maneuvers and the effects of disease.

#### Acknowledgments

This work was supported in part by NIH Grant RO1 AM 33923 and the Veterans Administration Medical Research Service. The authors would like to thank Ms. Lou Thurman for secretarial assistance, Bruce Kaplan for patient referral and scheduling, and Dr. Dominique Sappey-Marini, who was supported by a french government grant, for helpful discussions. The technical assistance by Mr. James Buchanan is gratefully acknowledged.

Reprint requests to Michael W. Weiner, M.D., Magnetic Resonance Unit (11M), VA Medical Center, 4150 Clement Street, San Francisco, California 94121, USA.

#### References

- CUNARRO JA, SCHULTZ SE, JOHNSON WA, WEINER MW: Effects of ischemia on metabolite concentrations in dog renal cortex. *Renal Physiol* 5:143–155, 1982
- SIEGEL NJ, AVISON MJ, REILLY HF, ALGER JR, SHULMAN RG: Enhanced recovery of renal ATP with postischemic infusion of ATP-MgCl<sub>2</sub> determined by  $^{31}\text{P}$ -NMR. *Am J Physiol* 245:F530–F534, 1983
- WOLFF SD, ENG C, BALABAN RS: NMR studies of renal phosphate metabolites in vivo: Effects of hydration and dehydration. *Am J Physiol* 255:F581–F589, 1988
- ROSS B, FREEMAN D, CHAN L: Contributions of nuclear magnetic resonance to renal biochemistry. *Kidney Int* 29:131–141, 1986
- WEINER MW, ADAM WR: Magnetic resonance spectroscopy for evaluation of renal function. (abstract) *Semin Urol* III:34, 1985
- CHAN L, FRENCH ME, GADIAN DG, MORRIS PJ, RADDA GK, BORE PJ, ROSS BD, STYLES P: Study of human kidneys prior to transplantation by phosphorous nuclear magnetic resonance, in *Organ Preservation III*, edited by PEGG DE, HALASZ NA, JACOBSEN I, Lancaster, MTP Press, 1981, p. 113–119
- SEHR PA, RADDA GK, BORE PJ, SELLS RA: A model kidney transplant studied by phosphorous nuclear magnetic resonance. *Biochem Biophys Res Commun* 77:195–202, 1977
- ACKERMAN JJH, LOWRY M, RADDA GK, ROSS BD, WONG GG: The role of intrarenal pH in regulation of ammoniogenesis:  $^{31}\text{P}$  NMR studies of the isolated perfused rat kidney. *J Physiol* 319: 65–80, 1981
- SHINE NR, XUAN JA, KORETSKY AP, WEINER MW: Determination of renal molar concentrations of phosphorus-containing metabolites in vivo using  $^{31}\text{P}$  NMR. *Magn Reson Med* 4:244–251, 1987
- CHAN L, LEDINGHAM JGG, DIXON JA, THULBORN KR, WATER-TON JC, RADDA GK, ROSS BD: Acute renal failure: A proposed mechanism based upon  $^{31}\text{P}$  nuclear magnetic resonance studies in the rat, in *Acute Renal Failure*, edited by ELIAHOU RE, London, J. Libbey, 1982, pp. 35–41
- SIEGEL NJ, GAUDIO KM, COOPER K, THULIN G, AVISON M, STROMSKI M, KASHGARIAN M, SHULMAN RG: Accelerating recovery from acute renal failure: Exogenous metabolite augmentation. *Mol Physiol* 8:593–598, 1985
- BALABAN RS, GADIAN DG, RADDA GK: Phosphorus nuclear magnetic resonance study of the rat kidney in vivo. *Kidney Int* 20:575–579, 1981
- AUE WP: Localization methods for in vivo nuclear magnetic resonance spectroscopy. *Rev Magn Reson Med* 1:21–72, 1986
- BOTTOMLEY PA, FOSTER TB, DARROW RD: Depth-resolved surface coil spectroscopy (DRESS) for in vivo  $^1\text{H}$ ,  $^{31}\text{P}$ , and  $^{13}\text{C}$  NMR. *J Magn Reson* 59:338–342, 1984
- GARWOOD M, SCHLEICH T, MATSON GB, ACOSTA G: Spatial localization of tissue metabolites by phosphorus-31 NMR rotating frame zeugmatography. *J Magn Reson* 60:268–279, 1984
- ORDIDGE RJ, CONNELLY A, LOHMAN JAB: Image-selected in vivo spectroscopy (ISIS). A new technique for spatially selective NMR spectroscopy. *J Magn Reson* 66:283–294, 1986
- BROWN TR, KINCAID BM, UGURBIL K: NMR chemical shift imaging in three dimensions. *Proc Natl Acad Sci (USA)* 79: 3523–3526, 1982
- MAUDSLEY AA, HILAL SK, PERMAN W, SIMON HE: Spatially resolved high resolution spectroscopy by “four dimensional” NMR. *J Magn Reson* 51:147–152, 1983
- BOTTOMLEY PA: Human in vivo NMR spectroscopy in diagnostic medicine: Clinical tool or research probe? *Radiology* 170:1–15, 1989
- WEINER MW: The promise of magnetic resonance spectroscopy for medical diagnosis. *Invest Radiol* 23:253–261, 1988
- LAWRY TJ, KARCZMAR GS, WEINER MW, MATSON GB: Computer simulation of MRS localization techniques: An analysis of ISIS. *Magn Reson Med* 9:299–314, 1989
- MATSON GB, TWIEG DB, KARCZMAR GS, LAWRY TJ, GOBER JR, VALENZA M, BOSKA MD, WEINER MW: Image-guided surface coil  $^{31}\text{P}$  MRS of human liver, heart, and kidney. *Radiology* 169:541–549, 1988
- MURPHY-BOSCH J, KORETSKY AP: An in vivo NMR probe circuit for improved sensitivity. *J Magn Reson* 54:526–532, 1983
- GORDON RE, TIMMS WE: An improved tune and match circuit for B<sub>0</sub> shimming in intact biological samples. *J Magn Reson* 46: 323–324, 1982
- PAN JW, HETHERINGTON HP, HAMM JR, ROTHMAN DL, BEHAR KL, SHULMAN RG: Volume localization with a single surface coil. *J Magn Reson* 81:608–616, 1989
- FRAHM J, MERBOLDT K-D, HAENICKE W: Localized proton spectroscopy using stimulated echoes. *J Magn Reson* 72:502–508, 1987
- FREEMAN DM, CHAN L, YAHAYA H, HOLLOWAY P, ROSS BD: Magnetic resonance spectroscopy for the determination of renal metabolic rate in vivo. *Kidney Int* 30:35–42, 1986
- MEYERHOFF DJ, KARCZMAR GS, MATSON GB, BOSKA MD, WEINER MW: Non-invasive quantitation of human liver metabolites using image-guided  $^{31}\text{P}$  Magnetic Resonance Spectroscopy. *NMR in Biomed* 3:17–22, 1990
- HRICAK H, NEWHOUSE JF: MR imaging of the kidney. *Radiol Clin N Am* 22:287–296, 1984
- COWGILL LD, MATSON GB, BOGUSKY RT: Application of  $^{31}\text{P}$ -Nuclear Magnetic Resonance to the study of renal phosphate excretion in vivo, in *Kidney Metabolism and Function*, edited by DZURIK R, LICHARDUS B, GUDER W, Boston, Martinus Nijhoff Publishers, 1985, pp. 256–264
- ACKERMANN JJH, GADIAN DG, RADDA GK, WONG GD: Observation of  $^1\text{H}$  NMR signals with receiver coils tuned to other nuclides. *J Magn Reson* 42:498–500, 1981
- SEGEARTH C, GRIVEGNEE A, LUYTEN PR, DEN HOLLANDER JA:  $^1\text{H}$  image-guided localized  $^{31}\text{P}$  MR spectroscopy of the human liver. *Magn Reson Med Biol* 1:7–16, 1988
- SEGEARTH C, BALERIAUX D, ARNOLD DL, LUYTEN PR, DEN HOLLANDER JA: Image-guided localized  $^{31}\text{P}$  MR spectroscopy of human brain tumors in situ: Effect of treatment. *Radiology* 165: 215–219, 1987

34. HEINDEL W, BUNKE J, GLATHE S, STEINBRICH W, MOLLEVANGER L: Combined <sup>1</sup>H-MR imaging and localized <sup>31</sup>P-spectroscopy of intracranial tumors in 43 patients. *J Comp Assit Tomogr* 12: 907-916, 1988
35. ROTH K, HUBESCH B, MEYERHOFF DJ, NARUSE S, GOBER JR, LAWRY TJ, BOSKA MD, MATSON GB, WEINER MW: Noninvasive quantitation of phosphorus metabolites in human tissue by NMR spectroscopy. *J Magn Res* 81:299-311, 1989
36. HUBESCH B, SAPPEY-MARINIER D, ROTH K, MEYERHOFF DJ, MATSON GB, WEINER MW: <sup>31</sup>P NMR spectroscopy of normal human brain and brain tumors. *Radiology* 174:401-409, 1990
37. MEYERHOFF DJ, BOSKA MD, THOMAS A, WEINER MW: Image-guided <sup>31</sup>P Magnetic Resonance Spectroscopy of alcoholic liver disease. *Radiology* 173:393-400, 1989
38. SCHAEFER S, GOBER JR, VALENZA M, KARZMAR G, MATSON GB, CAMACHO A, BCTVINICK EH, MASSIE B, WEINER MW: Magnetic resonance imaging guided <sup>31</sup>P-Phosphorus spectroscopy of the human heart. *J Am Coll Cardiol* 12:1449-1455, 1988
39. JUE T, ROTHMAN DL, LOHMAN JAB, HUGHES EW, HANSTOCK CC, SHULMAN RG: Surface coil localization of <sup>31</sup>P NMR signals from orthotopic human kidney and liver. *Proc Natl Acad Sci USA* 85:971-974, 1988
40. GRIST TM, KNEELAND JB, JESMANOWICZ A, FRONCISZ W, HYDE JS: *In vivo* MRI and localized <sup>31</sup>P MRS of the kidney in renal transplant recipients. (abstract) *Soc Magn Reson Med Book of Abstracts* 1:559, 1987
41. SHAPIRO JI, HAUG CE, SHANLEY PF, WEIL R III, CHAN L: <sup>31</sup>P Nuclear Magnetic Resonance study of renal allograft rejection in the rat. *Transplantation* 45:17-21, 1988
42. SHAPIRO JI, HAUG CE, WEIL R III, CHAN L: <sup>31</sup>P Nuclear Magnetic Resonance study of acute renal dysfunction in rat kidney transplants. *Magn Reson Med* 5:346-352, 1987
43. GYULAI L, BOLINGER L, LEIGH, JS JR, BARLOW C, CHANCE B: Phosphorylethanolamine—the major constituent of the phosphomonoester peak observed by <sup>31</sup>P-NMR on developing dog brain. *FEBS Lett* 178:137-142, 1984
44. SHAPIRO JI, CHAN L: <sup>31</sup>P Nuclear Magnetic Resonance study of obstructive uropathy in the rat. *J Clin Invest* 80:1422-1427, 1987
45. KORETSKY AP, WANG S, MURPHY-BOESCH J, KLEIN MP, WEINER MW: <sup>31</sup>P NMR spectroscopy of rat organs, in situ, using chronically implanted radiofrequency coils. *Proc Natl Acad Sci USA* 80: 7491-7495, 1983
46. RADDA GK, ACKERMAN JJH, BORE P, SEHR P, WONG GG, ROSS BD, GREEN Y, BARTLETT S, LOWRY M: <sup>31</sup>P NMR studies on kidney intracellular pH in acute acidosis. *Int J Biochem* 12:277-281, 1980
47. SEHR P, BORE P, PAPTAEOFANIS J, RADDA GK: Nondestructive measurement of metabolites and tissue pH in the kidney by <sup>31</sup>P nuclear magnetic resonance. *Br J Exp Pathol* 60:632-641, 1979
48. BARANY M, LANGER BG, GLICK RP, VENKATASUBRAMANIAN PN, WILBUR AC, SPIGOS DG: In-vivo H-1 spectroscopy in humans at 1.5 T. *Radiology* 167:839-844, 1988
49. HANSTOCK CC, ROTHMAN DL, PRICHARD JW, JUE T, SHULMAN RG: Spatially localized <sup>1</sup>H NMR spectra of metabolites in the human brain. *Proc Natl Acad Sci USA* 85:1821-1825, 1988
50. FRAHM J, BRUHN H, GYNGELL ML, MERBOLDT K-D, HAENICKE W, SAUTER R: Localized high-resolution proton NMR spectroscopy using stimulated echoes: Initial applications to human brain in vivo. *Magn Reson Med* 8:49-64, 1988
51. JUE T, LOHMAN JAB, ORDDIDGE RJ, SHULMAN RG: Natural abundance <sup>13</sup>C NMR spectroscopy of glycogen in humans. *Magn Reson Med* 5:377-379, 1987